

Shape Analysis and Classification of Masses in Mammographic Images using Neural Networks

Dijana Tralic, Jelena Bozek, Sonja Grgic

University of Zagreb, Faculty of Electrical Engineering and Computing

Department of Wireless Communications

Unska 3/XII, HR-10000 Zagreb, Croatia

Email: dijana.tralic@fer.hr

Abstract - Shape analysis of masses in mammographic images includes representation of mass contour and shape factors which are important features for distinguishing between benign and malignant masses. Three shape factors, namely compactness, moments and Fourier descriptors were calculated and used for the classification. Classification was performed using two types of neural networks: single layer and multilayer perceptron. Area under the ROC curve of $A_z = 0.9528$ was achieved using perceptron with 1000 epochs and using all shape factors. Multilayer perceptron with 1000 epochs and all shape factors achieved better classification results and area under the ROC curve of $A_z = 0.9988$.

Keywords - mammographic image; shape analysis; shape factors; classification; neural network

I. INTRODUCTION

Breast cancer is a major cause of death in women. If breast cancer is detected at an early stage, the survival rate can be dramatically increased. Currently the most effective method for the detection of early breast cancer in screening programs is X-ray mammography.

Mammographic images are analyzed by radiologists. Any feature that causes a departure from normal pattern or distortion with reference to the normal pattern is viewed with suspicion and analyzed with extra attention. Abnormalities such as calcifications, masses, architectural distortion and asymmetry between the left and right breast images are carefully analyzed. Masses are characterized with their density, margins and shape. Shape of a mass is one of the important features that helps distinguishing benign from malignant masses.

Cascio et al. [1] used features that give geometrical information and shape parameters for each region of interest to classify masses. They used supervised neural network which achieved area under the receiver operating characteristic (ROC) curve of $A_z = 0.862 \pm 0.007$ and sensitivity of 82%. Delogu et al. [2] used multilayer perceptron neural network to classify segmented mass using features based on shape, size and intensity of the segmented mass. They reported the area under ROC curve of $A_z = 0.805 \pm 0.030$ for correctly segmented masses. De Carvalho et al. [3] used the turning angle function for analyzing mass contour. They obtained classification accuracy of 0.92 in terms of area under the ROC curve.

Rangayyan et al. [4] combined three shape factors, spiculation index, fractional concavity and compactness and achieved classification accuracy of 81.5%. Overview and performance of other methods for mass classification is given by Rangayyan et al. [5].

This paper is organized as follows. In Section II the analysis of shape is explained. Computation of shape factors and classification using neural networks are presented in Section III. Obtained results are presented and discussed in Section IV. Section V draws the conclusion and gives some final remarks.

II. ANALYSIS OF SHAPE

Shape is one of key features in discriminating between normal and abnormal masses in the mammographic images. Most benign masses appear as well circumscribed areas with smooth boundaries that are circular or oval [6]. On the other hand, malignant masses have a rough shape with strands or spicules appearing to radiate from a central mass.

A. Representation and Signatures of Contours

The most common way of representing a contour is in terms of the coordinates of pixels along the contour [7]. Any contour with N points can be represented by the series of coordinates $\{x(n), y(n)\}$, $n = 0, 1, 2, \dots, N-1$.

The dimensionality of that representation can be reduced by computing distances from each contour point to a reference point. The center of mass is an appropriate reference, and its coordinates can be determined by

$$\bar{x} = \frac{1}{N} \sum_{n=0}^{N-1} x(n), \quad \bar{y} = \frac{1}{N} \sum_{n=0}^{N-1} y(n). \quad (1)$$

The signature of the contour is then defined as

$$d(n) = \sqrt{[x(n) - \bar{x}]^2 + [y(n) - \bar{y}]^2}, \quad (2)$$

and provides general information about the nature of the contour such as its smoothness or roughness. One of the problems of this approach is that the center of the mass of the concave regions or the regions with holes could lie outside the regions.

Another way to represent signature is through complex sequence $z(n) = x(n) + jy(n)$, where $n = 0, 1, 2, \dots, N-1$.

B. Shape Factors

Shape factors are small number of measures that are used to encode the nature or form of a contour. They must satisfy several properties, of which the most important are [7]:

- invariance to shift in spatial position,
- invariance to rotation,
- invariance to scaling.

We used three shape parameters that depend on shape characteristic and that can be used for shape modeling. These are: compactness, moments and Fourier descriptors.

Compactness, the first shape factor, is a simple measure of the efficiency of a contour to contain a given area, defined by

$$C_o = P^2/A, \quad (3)$$

where P is contour perimeter and A is area enclosed. The value of compactness is larger when the area contained by contour of given length is smaller. The definition of compactness is modified to restrict the range of parameter to interval $[0,1]$ as

$$cf = 1 - 4\pi A/P^2. \quad (4)$$

The second shape factor is defined with moments and describes shape roughness. One definition of moments is based upon a sequence $d(n)$ that represents the Euclidean distances between the center of mass and all of the points along the contour. The moment of the sequence $d(n)$ is defined as

$$m_p = \frac{1}{N} \sum_{n=0}^{N-1} [d(n)]^p \quad (5)$$

and the central moment is defined as

$$M_p = \frac{1}{N} \sum_{n=0}^{N-1} [d(n) - m_1]^p, \quad (6)$$

where p is the order of moments.

To form a set of shape features, Gupta and Srinath [8] selected following normalized low order moments

$$F_1 = (M_2)^{1/2}/m_1, \quad (7)$$

$$F_2 = M_3/(M_2)^{3/2}, \quad (8)$$

$$F_3 = M_4/(M_2)^2, \quad (9)$$

where m_1 is the first moment, and M_2 , M_3 and M_4 are the second-, the third- and the forth-order central moment, respectively.

Shen [9] showed that the variations in F_2 and F_3 for differing shape complexity are small and do not show a simple progression. In order to overcome these limitations F_2 and F_3 were modified as follows

$$F_2' = M_3^{1/3}/m_1, \quad (10)$$

$$F_3' = M_4^{1/4}/m_1. \quad (11)$$

As the contour becomes rougher, the fourth-order term in F_3' becomes much larger than the second-order term in F_1 , and a good indicator of shape roughness is the following measure

$$mf = F_3' - F_1 \quad (12)$$

Measure mf provides the desired invariance for a given contour type as well as the desired variation across the various shape categories.

Last shape factor used in this paper was based on Fourier descriptors. Given a sequence $z(n)$, it is possible to derive Fourier descriptors of the contour as

$$Z(k) = \frac{1}{N} \sum_{n=0}^{N-1} z(n) \exp\left[\frac{-2j\pi nk}{N}\right], \quad (13)$$

where $k = -N/2, \dots, -1, 0, 1, \dots, (N/2)-1$. The normalized Fourier descriptors $Z_o(k)$ are defined as

$$Z_o(k) = \begin{cases} 0, & k = 0; \\ \frac{Z(k)}{|Z(1)|}, & \text{otherwise,} \end{cases} \quad (14)$$

so that magnitudes are independent of position, size, orientation and starting point of the contour. A shape factor ff based upon the normalized Fourier descriptors was defined by Shen [9] as

$$ff = 1 - \frac{\sum_{k=-N/2+1}^{N/2} |Z_o(k)/|k||}{\sum_{k=-N/2+1}^{N/2} |Z_o(k)|}. \quad (15)$$

The advantage of this measure is that it is limited to the range $[0,1]$ and is not sensitive to noise.

III. METHODOLOGY

Shape factors were used for the analysis of a set of contours of benign and malignant breast masses. The dataset included 104 contours (59 benign and 45 malignant) from Rangayyan et al. [7] that were drawn on digitized mammograms by an expert radiologist.

Contours were divided into training and test sets. Training sets included 49 benign and 35 malignant masses. Test sets consist of 10 malign and 10 benign contours that were not included in training process.

A. Computation of Shape Factors

The first step in the shape analysis was an adequate representation of the contour in the form that is suitable for the calculation of shape measures. Therefore, the contour was recorded as a series of coordinates that represents points of contours. The starting point was located left of the center of the mass and movement was in clockwise direction. Center of the mass was calculated as mean value of all coordinate points that belong to the contour. After determining the signature of the contour and the center of the mass, they were used for calculating shape factors.

Shape factors were calculated for all contours in training sets. It was noticed that they have in general the distinction of reflecting lower values for circumscribed benign masses and higher values for spiculated malignant masses.

Table I shows the values of shape factors for different contours. The values of shape factors for most benign contours were in range $[0, 0.4]$ for cf , $[0, 0.06]$ for mf , and $[0, 0.3]$ for ff . Most of the malignant contours had values that lay outside of those ranges. However, some values of shape factors indicate that contours belong to wrong class.

TABLE I. VALUES OF SHAPE FACTORS

Contour	Type	Shape factors		
		cf	mf	ff
	benign	0.0666	0.0552	0.2184
	benign	0.1797	0.0460	0.2235
	benign	0.5942	0.0658	0.4246
	malignant	0.2345	0.0629	0.3112
	malignant	0.4633	0.0407	0.3635
	malignant	0.8987	0.0841	0.5915

B. Classification

Two types of neural networks were used for classification purposes: single layer perceptron and multilayer perceptron [10]. Single layer perceptron is the simplest kind of feedforward artificial neural network, i.e. a linear classifier. It contains one neuron and can be applied only to linearly separable sets. A multilayer perceptron (MLP) is a feedforward artificial neural network that consists of multiple layers of nodes in a directed graph, which is fully connected from one layer to the next. It is a modification of the standard perceptron, which can distinguish data that are not linearly separable.

Input values of neural networks can contain a combination of the value of compactness, moments and Fourier descriptors for contours in training sets. Accuracy of results depends on selected combination of input values and the parameters of the neural networks that are experimentally determined. For training purposes, following MLP's parameters were defined:

- activation function for hidden layer: *tansig*,
- error propagation function: *trainrp*,
- learning factor: 1,
- stopping factor: 0.001.

Number of epochs and number of neurons in hidden layer were not defined at the starting point. The goal of training was to determine best values for those parameters. After training process, classification was validated on test sets.

IV. RESULTS

The values of shape features were employed as inputs to the networks and contours were classified into two groups: benign or malignant. Classification was carried out on training and test sets for different combination of input values.

A. Single Layer Perceptron

Different combinations of input values (cf , mf and ff) were selected for classification purposes. Training data included combination of two or all three values of shape factors for all contours in training sets. Classification was carried out by putting training data in 2D or 3D space, and by moving decision plane. Fig. 1 depicts a 3D plot of the feature vectors for the classification used as the training data in case where all three parameters were selected. Most benign contours (marked with "o") are grouped on one side of plane, and most malignant (marked with "+") on the other side of plane. There are some contours that belong to the wrong side of plane, and classification of those contours could give inaccurate results.

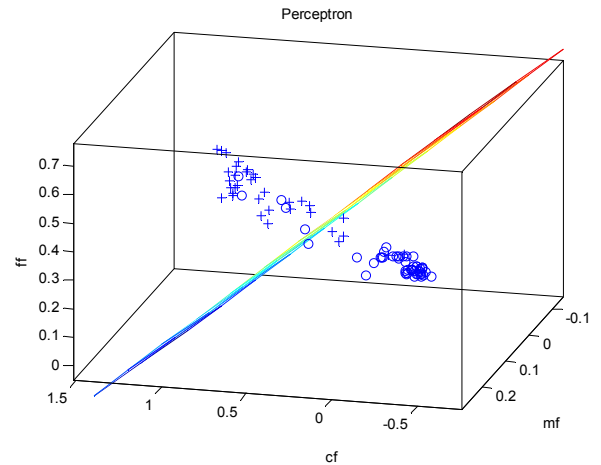


Figure 1. Training data

After selecting training data, number of epochs was experimentally defined, and the goal was to find value that gives the highest accuracy of results. Table II presents classification results for different combinations of shape factors and number of epochs. Results show that the combination of compactness and moments correctly classifies benign and malignant masses in almost 90% of cases, with only 100 epochs. However, the best results are accomplished by selecting all shape factors as input values. In that case, it is possible to detect benign and malignant masses with accuracy of 91.5 % (with 1000 epochs). Validation of results on the test sets showed that one benign and two malignant contours were incorrectly classified. Increasing number of epochs did not have much influence on the classification speed.

Accuracy of test has been assessed by receiver operating characteristic (ROC) curve, which plots the sensitivity (true positive rate, TPR) on y-axis versus 1-specificity (false positive rate, FPR) on x-axis. Fig. 2 presents fitted ROC curves for three cases of classification with different number of epochs, in case when all shape factors (cf , mf and ff) are calculated for training sets and used as input values to perceptron. Curves were fitted by applying rational function on empirical curves based on classification results. Analysis of curves indicates that higher number of epochs gives better accuracy. At the clinically important FPR range, ROC curves for 10 and 100 epochs are very similar. However, ROC curve for 1000 epochs demonstrates slightly lower sensitivity for range [0, 0.1], and significantly higher sensitivity for range [0.1, 0.2].

The performance was quantified using the area under the ROC curve, A_z , which was 0.9528 for the classification with 1000 epochs while for other two cases was 0.9446.

TABLE II. CLASSIFICATION WITH PERCEPTRON

Parameters	Epochs	Training sets		Test sets	
		<i>benign</i>	<i>malignant</i>	<i>benign</i>	<i>malignant</i>
$cf mf$	10	85,71%	85,71%	80%	70%
	100	87,75%	91,42%	80%	80%
$cf ff$	10	87,51%	82,85%	70%	70%
	100	89,79%	82,85%	80%	70%
$mf ff$	10	59,18%	77,15%	40%	60%
	100	87,75%	82,85%	80%	80%
$cf mf ff$	10	87,75%	85,71%	80%	70%
	100	89,79%	85,71%	80%	80%
	1000	91,84%	91,43%	90%	80%

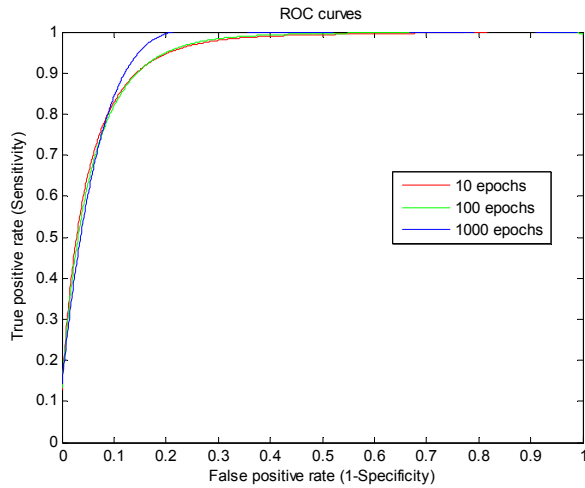


Figure 2. ROC curves for perceptron

B. Multilayer Perceptron

The same combination of input values used for single layer perceptron was applied on multilayer perceptron. The first problem was to determine number of hidden nodes, and experimental results showed that the best value was 50. Classification results for 50 nodes in hidden layer, and different combinations of input values and number of epochs are presented in Table III. Combination of moments and Fourier descriptors gives the worst results. It requires large number of epochs (5000) to accomplish good detection of contours in test sets (80%). Other combinations allow correct classification of malignant and benign training sets in almost 94% of cases, and in 80% of cases for tests sets (with 100 epochs).

Combination of all shape factors (cf , mf and ff) provided the best detection of contour's type. Number of epochs varied from 10 to 1500, but the best classification was accomplished with 1000 iterations. Accuracy of results was 100% for benign contours, and 97% for malignant contours in training sets.

Classification of contours in test sets was correct in 80% of cases, i.e. only two contours in every set were detected wrong. Further increase of number of epochs and neurons in hidden layer did not significantly influence the increase in classification accuracy. Duration of training stage was under 10 seconds for all combinations of input values, number of neurons and number of epochs.

ROC curves for multilayer perceptron classification with 50 hidden neurons, all shape factors (cf , mf and ff) and different number of epochs are presented on Fig. 3. Curves were fitted by applying exponential function on empirical curves. The most accurate classification was accomplished with 1000 epochs, where ROC curve is the most similar to perfectly accurate curve. This is due to the fact that network can learn to perfectly classify same set of data using sufficient number of epochs. The higher number of epochs would give perfect classification of contours in training sets, but accuracy of detection on test sets would become significantly lower.

The area under ROC curves indicates the same properties as ROC curves. The highest area is contained under the ROC curve for classification with 1000 epochs (0.9988). The area under the curve for 10 epochs is $A_z = 0.9294$ and for 100 epochs $A_z = 0.9732$.

TABLE III. CLASSIFICATION WITH MLP

Parameters	Epochs	Training sets		Test sets	
		<i>benign</i>	<i>malignant</i>	<i>benign</i>	<i>malignant</i>
$cf mf$	10	87,75%	94,29%	80%	80%
	100	93,88%	94,29%	80%	80%
$cf ff$	10	83,67%	94,29%	80%	80%
	100	93,88%	94,29%	80%	80%
$mf ff$	10	53,06%	100%	0%	100%
	100	89,79%	94,87%	100%	0%
$cf mf ff$	10	87,76%	94,29%	70%	80%
	100	91,83%	94,29%	80%	60%
	1000	100%	97,14%	80%	80%

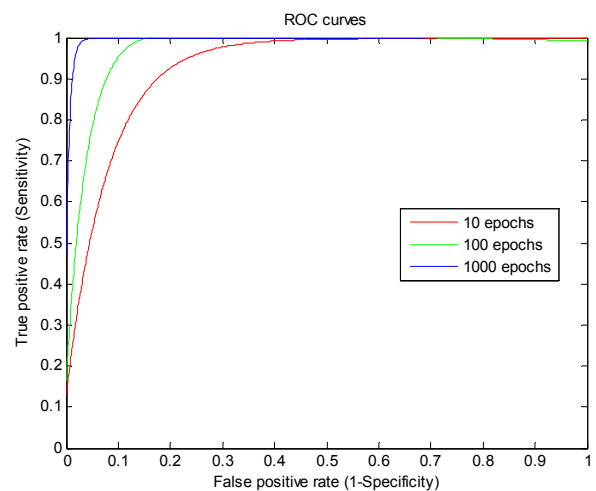


Figure 3. ROC curves for MLP

V. CONCLUSION

Shape factors based on compactness, moments and Fourier descriptors showed satisfactory properties for describing contour's features. Values of those shape factors were lower for oval benign masses and higher for spiculated malignant masses. Classification results indicated that they can be used for detection of malignant and benign masses in mammographic images.

Multilayer perceptron can learn to perfectly classify given data with appropriate number of epochs. For that reason, accuracy of results for training sets was higher when classification was carried out with multilayer perceptron, compared to single layer perceptron. However, classification of test sets indicated that single layer perceptron allows correct classification for higher number of contours.

Classification error existed in both cases, because some contours from benign class had shape characteristics of malignant class (and vice versa). The inclusion of measures representing other image characteristics (like texture or gradient) could complement shape factors and assist in improved analysis of masses.

ACKNOWLEDGMENT

The work described in this paper was conducted under the research projects: "Picture Quality Management in Digital Video Broadcasting" (036-0361630-1635) and "Intelligent Image Features Extraction in Knowledge Discovery Systems" (036-0982560-1643), supported by the Ministry of Science, Education and Sports of the Republic of Croatia.

REFERENCES

- [1] D. Cascio, F. Fauci, R. Magro, G. Raso, R. Bellotti, F. De Carlo, S. Tangaro, G. De Nunzio, M. Quarta, G. Forni, A. Lauria, M. E. Fantacci, A. Retico, G. L. Masala, P. Oliva, S. Bagnasco, S. C. Cheran, E. Lopez Torres, Mammogram Segmentation by Contour Searching and Mass Lesions Classification with Neural Network, *IEEE Transactions on Nuclear Science*, Vol. 53, No. 5, October 2006, pp. 2827-2833
- [2] P. Delogu, M. E. Fantacci, P. Kasae, A. Retico, Characterization of Mammographic Masses Using a Gradient-Based Segmentation Algorithm and a Neural Classifier, *Computers in Medicine and Biology*, Vol. 37, No. 10, October 2007, pp. 1479-1491
- [3] J. D. de Carvalho, D. Guliato, S. A. Santiago, R. M. Rangayyan, Polygonal Modeling of Contours Using the Turning Angle Function, *Canadian Conference on Electrical and Computer Engineering*, Vancouver, April 2007, pp. 1090-1093
- [4] R. M. Rangayyan, N. R. Mudigonda, J. E. L. Desautels, Boundary Modelling and Shape Analysis Methods for Classification of Mammographic Masses, *Medical and Biological Engineering and Computing*, Vol. 38, No. 5, 2000, pp. 487-496
- [5] R. M. Rangayyan, F. J. Ayres, J. E. L. Desautels, A Review of Computer-Aided Diagnosis of Breast Cancer: Toward the Detection of Subtle Signs, *Journal of the Franklin Institute*, Vol. 344, No. 3-4, 2007, pp. 312-348
- [6] E. S. de Paredes, *Atlas of Mammography*, 3rd Edition, Lippincott Williams & Wilkins, 2007
- [7] R. M. Rangayyan, *Biomedical Image Analysis*, CRC, 2005
- [8] L. Gupta, M. D. Srinath, Contour Sequence Moments for the Classification of Closed Planar Shapes, *Pattern Recognition*, Vol. 20, No. 3, 1987, pp. 267-272
- [9] L. Shen, R. M. Rangayyan, J. E. L. Desautels, Application of Shape Analysis to Mammographic Calcifications, *IEEE Transactions on Medical Imaging*, Vol. 13, No. 2, June 1994, pp. 263-274
- [10] S. Haykin, *Neural Networks A Comprehensive Foundation*, Prentice Hall International, New Jersey, 1999